

Convergence of direct and indirect methods in the magnetocaloric study of first order transformations: The case of Ni-Co-Mn-Ga Heusler alloys

G. Porcari,^{1,*} F. Cugini,¹ S. Fabbrici,^{2,3} C. Pernechele,¹ F. Albertini,³ M. Buzzi,^{1,†} M. Mangia,⁴ and M. Solzi¹

¹*Dipartimento di Fisica and CNISM, Università di Parma, viale G. P. Usberti 7/A, I-43100 Parma, Italy*

²*MIST E-R Laboratory, via Gobetti 101, I-40129 Bologna, Italy*

³*IMEM-CNR, Parco Area delle Scienze 37/A, I-43100 Parma, Italy*

⁴*BioPharmaNet, Department of Pharmacy, University of Parma, viale G. P. Usberti 27/A, Parma, Italy*

(Received 10 July 2012; published 27 September 2012)

The study of two aspects of the magnetocaloric effect (MCE), namely, the matching between isothermal entropy change and direct adiabatic temperature change, is not straightforward since huge differences between these two quantities have often been reported. Here we put in relation the direct and indirect measurements on the first order magnetostructural martensitic transformation occurring in Ni-Co-Mn-Ga alloys. In order to complete the characterization of the MCE and to find an explanation of these mismatches, differential scanning calorimeter measurements have been performed at different applied magnetic fields.

DOI: [10.1103/PhysRevB.86.104432](https://doi.org/10.1103/PhysRevB.86.104432)

PACS number(s): 75.30.Sg, 75.50.Cc

Solid-state magnetic refrigerators, besides being more environmentally friendly compared to existing technologies, are expected to show higher efficiencies.¹ This kind of device should be able to exchange heat faster than existing systems by operating the thermodynamic cycles at higher frequencies.² This technology is founded on the magnetocaloric effect (MCE), which appears as an isothermal entropy change (Δs_T) or an adiabatic temperature variation (ΔT_{ad}) induced by an applied magnetic field.^{1,3} Magnetic phase transitions are the regions where this effect is maximum. Since the discovery of the giant effect⁴ (GMCE) of $\text{Gd}_5\text{Si}_2\text{Ge}_2$, the MCE has been deeply investigated in materials showing first order magnetic transformations.⁵⁻⁸

The recently reported⁹ huge effect on Co-substituted Ni-Mn-based Heuslers is going to revitalize this research area. The effect reported on these systems turns out to be comparable to the best values of Gd-Si-Ge and La-Fe-Si-H alloys, thus attesting that Ni-Mn-based alloys are reliable materials for future power conversion devices. Heusler alloys, besides being rare-earth free, are characterized by a first order magnetostructural martensitic transformation.¹⁰ The magnetic properties and the critical temperature of this process can be easily tuned by properly varying the stoichiometry.¹¹

The study of the MCE near first order processes is not straightforward, even if its thermodynamic behavior has been carefully analyzed.^{1,3,12} As an example, the observation of artifact values while calculating Δs_T from isothermal $M(H)$ curves has often been reported.^{13,14} Though in some cases these anomalous values have been explained as effects of hysteresis,¹⁵ the proper application of the Maxwell relation to these processes is still under debate.^{12,16-18} Another important issue is the analysis of the different contributions to the total magnetic-field-induced¹⁹ Δs_T , taking into account the particular nature of the first order magnetic transformation.²⁰

Moreover, a reliable correlation between the Δs_T peak values and the ΔT_{ad} is even more difficult to find. Several works²¹⁻²⁵ report large differences between the directly measured ΔT_{ad} values, which are usually smaller, and the ΔT_{ad} values indirectly deduced from calorimetric and magnetization

measurements. The origin of these mismatches is difficult to grasp because the specific heat (c_p) of the materials is temperature and magnetic field dependent. This quantity, which is characterized by a complex behavior across a first order process, is the term relating the two aspects of the MCE:^{1,3} $dT_{ad} = (T/c_p)ds_T$. For this reason, a study of both of these properties (Δs_T and ΔT_{ad}) should always be performed when analyzing the magnetocaloric behavior of a material, together with a proper evaluation of the experimental errors.^{12,26}

The aim of this work is to study the behavior of the MCE near a first order process in a model system, trying to understand the correlations between ΔT_{ad} and Δs_T . The three main properties [$c_p(T, H)$, $\Delta T_{ad}(T, \Delta H)$, $\Delta s_T(T, \Delta H)$] are independently measured using a properly made in-field differential scanning calorimeter (DSC), suitable in the case of first order transformations,²⁷ a direct adiabatic temperature change probe, and magnetic characterization, respectively. Moreover, an estimation of the $\Delta T_{ad}(T, \Delta H)$ from $\Delta s_T(T, \Delta H)$ calculated from isothermal $M(H)$ measurements is presented using a geometrical model already discussed in a previous work.²⁸ In this model, the order parameter of the process is the transformed phase fraction. This approach seems to be a promising route to correlate the indirect $\Delta s_T(T, \Delta H)$ with the directly measured $\Delta T_{ad}(T, \Delta H)$ across first order processes: a similar idea has been recently presented in Ref. 9 leading to a good agreement. The whole discussion is complemented by an evaluation of the measurement errors following the treatment reported in Ref. 29.

It has to be noted that different techniques generally require a proper sample mass to optimize their specific signal-to-noise ratio. However, when comparing these results on materials undergoing first order transformations, the use of distinct samples could lead to different values, due to aging effects, thermomagnetic history, and different microstructural features.²¹ To avoid this problem, our experimental setups have been suitably designed to allow for the complete characterization on the same sample mass. This method has been tested on several samples: for the sake of simplicity, here we present one example.

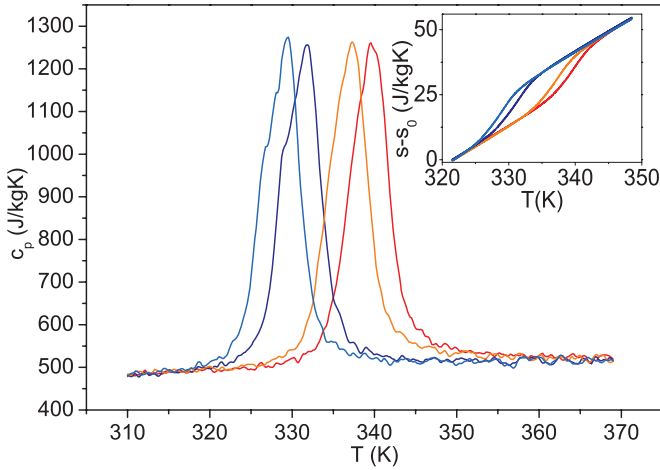


FIG. 1. (Color online) $c_p(T, H)$ and $s(T, H)$ (in the inset) curves performed on heating (red and orange lines; right-hand side) and on cooling (dark blue and light blue lines; left-hand side) in $\mu_0 H = 0$ T and $\mu_0 H = 1.8$ T for the sample $\text{Ni}_{44.83}\text{Co}_{4.77}\text{Mn}_{32.15}\text{Ga}_{18.25}$.

This study will be performed on a Ni-Co-Mn-Ga Heusler characterized by a magnetostructural hysteretic transformation at 340 K on heating in zero field. This material shows inverse MCE,³⁰ across a nearly steplike martensitic transformation, and is thus an ideal candidate in order to study the MCE across a first order process. The sample $\text{Ni}_{44.83}\text{Co}_{4.77}\text{Mn}_{32.15}\text{Ga}_{18.25}$ was prepared by arc melting the stoichiometric amounts of pure elements and was subsequently homogenized by annealing at 900 °C for 72 h. Magnetic measurements were performed using a Quantum Design Inc. MPMS SQUID magnetometer, according to a previously described protocol.²⁸ Direct ΔT_{ad} was measured by using a homemade probe based on a Cernox HT-BR temperature sensor²⁸ in an electromagnet with a maximum field rate of ~ 2 T/s up to 1.90 ± 0.05 T. In this case, the error (± 0.15 K) is due to the sensor electric noise and corresponds to its resistance resolution of $\pm 0.01\Omega$. The DSC in-field curves were performed in a homemade Peltier cell calorimeter able to work in 10^{-5} mbar vacuum between 255 and 400 K. Its temperature control resolution is ± 0.01 K and the thermal sweep is controlled by a high-power Peltier cell, exploiting solutions similar to those proposed in Refs. 31 and 32. The calibration was performed with a single crystal sapphire sample and the reliability of the measurements was verified by measuring samples of copper and molybdenum and testing the latent heat of the fusion of gallium. These measurements have also been compared with those performed on a commercial DSC 821 Mettler Toledo driven by STAR^e software. The errors of the MCE obtained from the calorimetric DSC measurements will be discussed in the following. The magnetic field reported throughout the paper is the external one: the effective internal field at saturation has been estimated to be ~ 0.16 T lower due to demagnetizing effects in the case of cubic samples.

In Fig. 1, calorimetric isofield curves at $\mu_0 H = 0$ T and $\mu_0 H = 1.8$ T for the Ni-Co-Mn-Ga sample both in heating and cooling are shown. Three features can be immediately noticed: (i) a c_p value near 300 K slightly lower than 500 J/kg K, which is typical of this kind of alloy; (ii) a thermal hysteresis of ~ 8 K both in-field and in zero field; and

(iii) the inverse MCE is confirmed by the negative shift of the transformation temperature when $H \neq 0$. We have verified that at least for a thermal sweep rate of 0.04 K/s, the kinetic correction³² to the DSC $c_p(T, H)$ curves can be neglected. The entropy curves calculated²⁹ from $c_p(T, H)$ are displayed in the inset of Fig. 1.

Recently it has been underlined how the hysteresis can affect the MCE while the external magnetic field is cycled across first order transformations.³³ It can be observed from Fig. 1 that this material could not be used in a real refrigeration cycle. In the present case, the large hysteresis, if compared to the martensitic temperature shift induced by the external applied field, would prevent the reversal of the transformation during the demagnetizing process. This work is focused on the correlation between the information that can be deduced from the three main techniques of investigation of the MCE across first order processes by understanding if some of these measurements can lead to over- or underestimations of the phenomenon, carefully evaluating the error associated with every technique. For this reason, only the first cycle of the heating branch of the process will be analyzed.

Isofield $M(T)$ curves (inset of Fig. 2) confirm the occurrence of the martensitic transformation in zero field at 340 K and the entity of the shift induced by the applied field $\Delta T_{M-A} = -2.4 \pm 0.4$ K in $\mu_0 \Delta H = 1.8$ T, in agreement with the calorimetric measurements of Fig. 1. Moreover, from the same curves, $\Delta M = 16 \pm 1$ Am²/kg values can be deduced, together with an estimation of the Clausius-Clapeyron $\Delta s_T \sim 11.5$ J/kg K. Both martensite and austenite in this sample are ferromagnetic phases leading to a relatively small ΔM jump across the first order process with respect to other compositions.³⁰ Isothermal $M(H)$ magnetization measurements (Fig. 2) show a continuous behavior, and thus their integration to obtain the magnetic-field-induced Δs_T is analytically allowed.^{13,34} $M(H)$ curves, in order to avoid artifact values while calculating the Δs_T , have been measured, taking care to cross the cooling branch of the martensitic transformation after every field sweep.²⁸

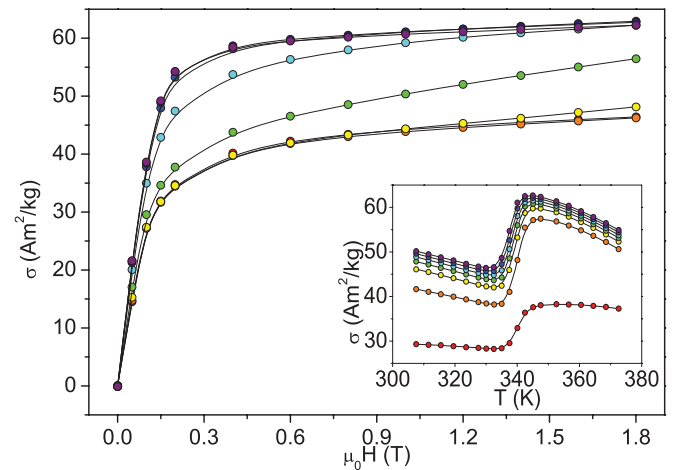


FIG. 2. (Color online) Isothermal and isofield (inset) measurements. The $M(H)$ curves were taken at intervals of 3 K from 320 to 350 K.

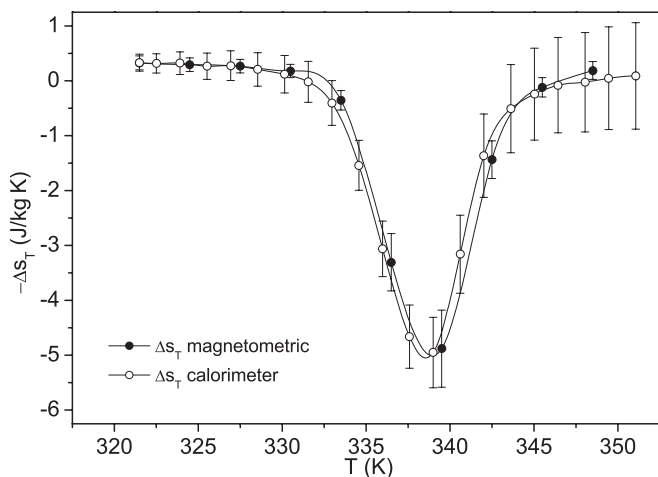


FIG. 3. Δs_T on heating obtained from calorimetric and magnetometric measurements using the Maxwell relation.

The isothermal entropy change obtained from $c_p(T, H)$ and $M(H)$ curves is reported in Fig. 3. The calorimetric Δs_T is deduced subtracting the entropy curve at $\mu_0 H = 0$ T from the one at $\mu_0 H = 1.8$ T (inset of Fig. 1) following Eq. (1):

$$\Delta s_T(T, \mu_0 \Delta H) = \Delta s_T(T_i, \mu_0 \Delta H) + \int_{T_i}^T \frac{c_p(T, H_2) - c_p(T, H_1)}{T} dT, \quad (1)$$

where $\Delta H = H_2 - H_1$ and T_i is the reference starting temperature, in the region far below the transformation. $\Delta s_T(T_i, \mu_0 \Delta H) = -0.33 \pm 0.15$ J/kg K is a correction, corresponding to a slight vertical shift of the in-field entropy curve at $T_i = 321.5$ K, which is required³² since the integration starting temperature is above 0 K. This $\Delta s_T(T_i, \mu_0 \Delta H)$, obtained from Maxwell elaboration of isothermal $M(H)$ curves, is a value reported also for other compositions^{28,32,35} in a field span of $\mu_0 \Delta H \sim 2$ T and it is due to the magnetic contribution of the martensite. This correction consists in less than $\sim 7\%$ of the peak value. The effective error on the MCE deduced by the calorimetric technique has been verified in our case to be due to slightly different vacuum conditions between the in-field and the zero field $c_p(T, H)$ curves. This effect constitutes the mean error on the specific heat of our experimental setup. It has been verified to be within 0.7% and it leads in this case to an uncertainty of $\sim 13\%$ on the Δs_T peak value (see Fig. 3). Both the in-field and zero-field entropy curves are thus affected by an effective relative error of the order of 0.7%, while for the in-field curve, an additional constant error of ± 0.15 J/kg K has been considered. These assumptions have then been applied to the standard method of Ref. 29 in order to calculate the final error.

The calorimetric Δs_T curve (Fig. 3) reaches a maximum value of 4.95 ± 0.64 J/Kg K at ~ 339 K. Its shape matches the Maxwell derived one, while the peak values are in good agreement within their uncertainty. The error bars of the magnetometric Δs_T data turn out to be $\sim 15\%$.

As already discussed, a discrepancy is often reported between the ΔT_{ad} values obtained by direct techniques and indirectly deduced from magnetometric or calorimetric methods.^{21–24} In the present case, a previously described

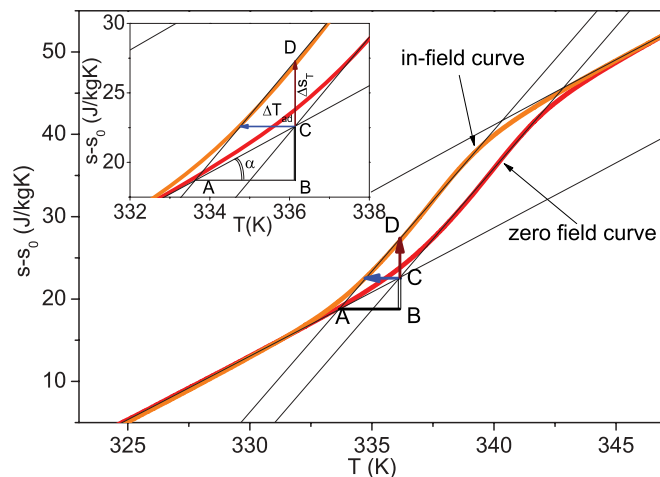


FIG. 4. (Color online) Real heating calorimetric $s(T, H)$ curves across the transformation. The geometrical construction, which correlates the different properties of the first order process, has been superimposed on them. Inset: enlarged view.

model²⁸ is used to calculate the ΔT_{ad} on the basis of purely magnetometric measurements and it is compared with direct values. In Fig. 4, the geometrical construction that correlates direct and indirect measurements has been superimposed on the calorimetric heating curves. It can be seen that the model matches the real situation since $A_{s-H_1} < A_{f-H_2}$, where A_{s-H_1} (austenite start in $\mu_0 H_1 = 0.1$ T) and A_{f-H_2} (austenite finish in $\mu_0 H_2 = 1.8$ T) are taken as the second order derivative peaks of the isofield $M(T)$ curves²⁸ (Fig. 2). In this case, $\tan \alpha \sim \frac{c_p}{T} = 1.5 \pm 0.1$ J/kg K² is considered, while $AB = A_{s-H_2} - A_{s-H_1} = 2.5 \pm 0.4$ K. The estimation of the adiabatic temperature change comes then from the relation (see Fig. 4) $AB : \Delta T_{ad} = (\Delta s_T + CB) : \Delta s_T$.

In Fig. 5, the different adiabatic temperature change curves, i.e., directly measured ones, calculated from magnetometric Δs_T values and obtained from calorimetric data, are compared. The matching between the results of different techniques is evident both from the peak values and from the shape

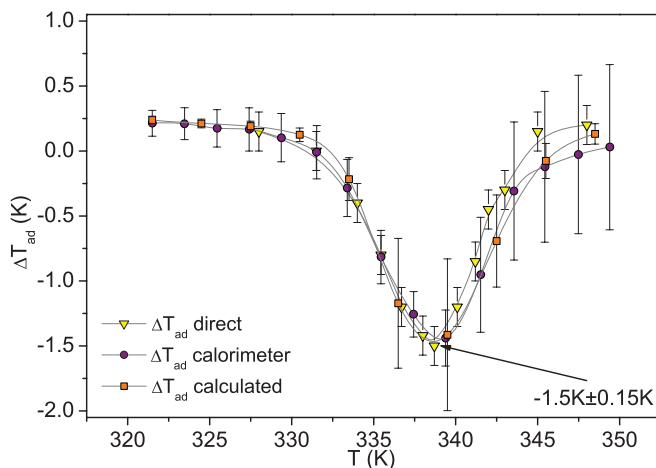


FIG. 5. (Color online) Cross characterization of ΔT_{ad} , directly measured (yellow triangles), obtained from c_p data (violet circles), and calculated from Δs_T values (orange squares).

of the curves. The three measurements converge to $\Delta T_{\text{ad}} = -1.45 \pm 0.05$ K (Fig. 5). The calorimetric ΔT_{ad} and its error have been calculated following the treatment of Ref. 29. The corresponding error bars after the transition appear consistent as a consequence of the error propagation on Eq. (1). This behavior is in good agreement with some results already reported in the literature.²⁹ The errors on the direct ΔT_{ad} measurement are the same all over the curve since they depend on the resistance resolution of the sensor, which is constant. The peak value calculated by means of the model of Fig. 4 is affected by a larger error since it follows from multiple elaboration of $M(H)$ data.

In conclusion, it has been shown that the results of the three techniques converge to the same values within the experimental errors by using a rigorous experimental protocol.

This study of separately measuring $\Delta S_T(T, \Delta H)$, $\Delta T_{\text{ad}}(T, \Delta H)$, and $c_p(T, H)$ is possible through the development of two *ad hoc* experimental setups. In order to mitigate the inherent drawbacks of the first order process due to different aging effects, microstructural defects, and thermomagnetic histories, the whole characterization has been performed on the same sample. This particular issue, if neglected, could be one of the main sources of uncertainty when comparing

different aspects of the MCE. A thorough error treatment makes it possible to evaluate the reliability of each technique and qualifies the comparison of the same property obtained from different methods. The converging results confirm the suitability of Maxwell elaboration of isothermal $M(H)$ curves also in the case of first order processes.²⁷

A model, which is based on magnetization data, has been proposed and allows one to estimate ΔT_{ad} from $M(H)$ measurements. Its simplicity and the need for standard magnetization measurements and a single value of the specific heat away from the transformation make this model a powerful tool for a reliable qualitative estimation of the ΔT_{ad} . Nonetheless, the direct measurement remains the more accurate technique to obtain the ΔT_{ad} . Other considerations that follow from this study involve the kinetics of the martensitic transformation. The concurrent application of techniques characterized by different time scales (from $\sim 10^{-3}$ to ~ 2 T/s) to the same process has led to very similar results. This could support the hypothesis that in these systems, the fast field sweep rates that are applied while performing the direct measurement should not compete with the kinetics of the martensitic transformation, in agreement with previous studies.²²

*giacomo.porcari@fis.unipr.it

[†]Present address: Swiss Light Source, Paul Scherrer Institut, CH-5232 Villigen, Switzerland.

¹A. M. Tishin and Y. I. Spichkin, *The Magnetocaloric Effect and its Applications* (Institute of Physics, Bristol, 2003).

²A. Kitanovski and P. Egolf, *Int. J. Refrig.* **33**, 449 (2010).

³V. K. Pecharsky, K. A. Gschneidner Jr., A. O. Pecharsky, and A. M. Tishin, *Phys. Rev. B* **64**, 144406 (2001).

⁴V. K. Pecharsky and K. A. Gschneidner Jr., *Phys. Rev. Lett.* **78**, 4494 (1997).

⁵A. Fujita, S. Fujieda, Y. Hasegawa, and K. Fukamichi, *Phys. Rev. B* **67**, 104416 (2003).

⁶H. Wada and Y. Tanabe, *Appl. Phys. Lett.* **79**, 3302 (2001).

⁷L. Pareti, M. Solzi, F. Albertini, and A. Paoluzi, *Eur. Phys. J. B* **32**, 303 (2003).

⁸O. Tegus, E. Brück, K. H. J. Buschow, and F. R. de Boer, *Nature (London)* **415**, 150 (2002).

⁹J. Liu, T. Gottschall, K. P. Skokov, J. D. Moore, and O. Gutfleisch, *Nature Mater.* **11**, 620 (2012).

¹⁰A. Planes, L. Mañosa, and M. Acet, *J. Phys.: Condens. Matter* **21**, 233201 (2009).

¹¹S. Fabbri, F. Albertini, A. Paoluzi, F. Bolzoni, R. Cabassi, M. Solzi, L. Righi, and G. Calestani, *Appl. Phys. Lett.* **95**, 022508 (2009).

¹²N. A. de Oliveira and P. J. von Ranke, *Phys. Rev. B* **77**, 214439 (2008).

¹³L. Caron, Z. Q. Ou, T. T. Nguyen, D. T. Cam Thanh, O. Tegus, and E. Brück, *J. Magn. Magn. Mater.* **321**, 3559 (2009).

¹⁴S. Das, J. S. Amaral, and V. S. Amaral, *J. Phys. D: Appl. Phys.* **43**, 152002 (2010).

¹⁵V. Basso, C. P. Sasso, K. P. Skokov, O. Gutfleisch, and V. V. Khovaylo, *Phys. Rev. B* **85**, 014430 (2012).

¹⁶A. Magnus, G. Carvalho, A. A. Coelho, P. J. von Ranke, and C. S. Alves, *J. Alloys Compd.* **509**, 3452 (2011).

¹⁷J. S. Amaral and V. S. Amaral, *J. Magn. Magn. Mater.* **322**, 1552 (2010).

¹⁸W. Cui, W. Liu, and Z. Zhang, *Appl. Phys. Lett.* **96**, 222509 (2010).

¹⁹K. Morrison, J. Lyubina, J. D. Moore, A. D. Caplin, K. G. Sandeman, O. Gutfleisch, and L. F. Cohen, *J. Phys. D: Appl. Phys.* **43**, 132001 (2010).

²⁰K. Morrison, M. Bratko, J. Turcaud, A. Berenov, A. D. Caplin, and L. F. Cohen, *Rev. Sci. Instrum.* **83**, 033901 (2012).

²¹K. A. Gschneidner Jr., V. K. Pecharsky, and A. O. Tsokol, *Rep. Prog. Phys.* **68**, 1479 (2005).

²²V. V. Khovaylo, K. P. Skokov, Y. S. Koshkidáko, V. V. Koledov, V. G. Shavrov, V. D. Buchelnikov, S. V. Taskaev, H. Miki, T. Takagi, and A. N. Vasiliev, *Phys. Rev. B* **78**, 060403 (2008).

²³X. Moya, L. Manosa, A. Planes, S. Aksoy, M. Acet, E. F. Wassermann, and T. Krenke, *Phys. Rev. B* **75**, 184412 (2007).

²⁴V. K. Sharma, M. K. Chattopadhyay, R. Kumar, T. Ganguli, P. Tiwari, and S. B. Roy, *J. Phys.: Condens. Matter* **19**, 496207 (2007).

²⁵S. Fujieda, Y. Hasegawa, A. Fujita, and K. Fukamichi, *J. Magn. Magn. Mater.* **272**, 2365 (2004).

²⁶V. K. Pecharsky and K. A. Gschneidner Jr., *J. Appl. Phys.* **86**, 6315 (1999).

²⁷L. Mañosa, A. Planes, and X. Moya, *Adv. Mater.* **21**, 3725 (2009).

²⁸G. Porcari, S. Fabbri, C. Pernechele, F. Albertini, M. Buzzi, A. Paoluzi, J. Kamarad, Z. Arnold, and M. Solzi, *Phys. Rev. B* **85**, 024414 (2012).

²⁹V. K. Pecharsky and K. A. Gschneidner Jr., *J. Appl. Phys.* **86**, 565 (1999).

- ³⁰S. Fabbrici, J. Kamarad, Z. Arnold, F. Casoli, A. Paoluzi, F. Bolzoni, R. Cabassi, M. Solzi, G. Porcari, C. Pernechele, and F. Albertini, *Acta Mater.* **59**, 412 (2011).
- ³¹S. Jeppesen, S. Linderoth, N. Pryds, L. Theil Kuhn, and J. Buch Jensen, *Rev. Sci. Instrum.* **79**, 083901 (2008).
- ³²V. Basso, C. P. Sasso, and M. Küpferling, *Rev. Sci. Instrum.* **81**, 113904 (2010).
- ³³K. P. Skokov, V. V. Khovaylo, K. H. Müller, J. D. Moore, J. Liu, and O. Gutfleisch, *J. Appl. Phys.* **111**, 07A910 (2012).
- ³⁴K. A. Gschneidner Jr., V. K. Pecharsky, E. Bruck, H. G. M. Duijn, and E. M. Levin, *Phys. Rev. Lett.* **85**, 4190 (2000).
- ³⁵V. V. Khovaylo, K. P. Skokov, O. Gutfleisch, H. Miki, T. Takagi, T. Kanomata, V. V. Koledov, V. G. Shavrov, G. Wang, E. Palacios, J. Bartolomé, and R. Burriel, *Phys. Rev. B* **81**, 214406 (2010).